

Predictive Semi-Empirical NO_x Model for Diesel Engine

Saurabh Sharma, Yong Sun, Bruce Vernham

Abstract—Accurate prediction of NO_x emission is a continuous challenge in the field of diesel engine-out emission modeling. Performing experiments for each conditions and scenario cost significant amount of money and man hours, therefore model-based development strategy has been implemented in order to solve that issue. NO_x formation is highly dependent on the burn gas temperature and the O₂ concentration inside the cylinder. The current empirical models are developed by calibrating the parameters representing the engine operating conditions with respect to the measured NO_x. This makes the prediction of purely empirical models limited to the region where it has been calibrated. An alternative solution to that is presented in this paper, which focus on the utilization of in-cylinder combustion parameters to form a predictive semi-empirical NO_x model. The result of this work is shown by developing a fast and predictive NO_x model by using the physical parameters and empirical correlation. The model is developed based on the steady state data collected at entire operating region of the engine and the predictive combustion model, which is developed in Gamma Technology (GT)-Power by using Direct Injected (DI)-Pulse combustion object. In this approach, temperature in both burned and unburnt zone is considered during the combustion period i.e. from Intake Valve Closing (IVC) to Exhaust Valve Opening (EVO). Also, the oxygen concentration consumed in burnt zone and trapped fuel mass is also considered while developing the reported model. Several statistical methods are used to construct the model, including individual machine learning methods and ensemble machine learning methods. A detailed validation of the model on multiple diesel engines is reported in this work. Substantial numbers of cases are tested for different engine configurations over a large span of speed and load points. Different sweeps of operating conditions such as Exhaust Gas Recirculation (EGR), injection timing and Variable Valve Timing (VVT) are also considered for the validation. Model shows a very good predictability and robustness at both sea level and altitude condition with different ambient conditions. The various advantages such as high accuracy and robustness at different operating conditions, low computational time and lower number of data points requires for the calibration establishes the platform where the model-based approach can be used for the engine calibration and development process. Moreover, the focus of this work is towards establishing a framework for the future model development for other various targets such as soot, Combustion Noise Level (CNL), NO₂/NO_x ratio etc.

Keywords—Diesel engine, machine learning, NO_x emission, semi-empirical.

I. INTRODUCTION

ONE of the primary responsibilities while developing a diesel engine is the improvement in the emission

reduction from diesel engines along with the improvement in the fuel efficiency. Due to stringent emission norms OEMs have to focus on introducing new and better emission reduction techniques. As the US Environmental Protection Agency (EPA) and California Air Resources Board (CARB) are working towards low NO_x regulation, which will lead to the 90% reduction in NO_x regulatory limit from 0.2 g/bhp-hr to 0.02 g/bhp-hr. This will affect the OEMs very hard as they have to introduce latest technology in order to reach this goal. There is no doubt that the after-treatment systems are the most reliable and effective way to match the strict emission regulations, given that those systems are working in the region which is suitable for lit off and high conversion efficiency. But the high cost associated with these after-treatments incite OEMs to shift their focus on the pre-existing sophisticated advanced technology such as injection strategies, EGR process and turbocharging systems to reduce the engine-out emissions. In order to implement these technologies, model-based development (MBD) approach to perform the calibration has received lot of interest in past few years [1]. The reason for so much interest in the usage of MBD approach is that it requires fewer experimental efforts, hence reducing development time. Also, the MBD approach is capable of taking into the account of different ambient conditions (sea level, altitude levels etc.) and the variation in the parameters related to the engine operating conditions (EGR, injection timing, rail pressure etc.). These advantages provided by MBD approach drives the OEMs to use this approach to build 0D/1D predictive combustion and emissions model to perform future development work.

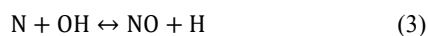
The presented work in this paper is a part of an MBD approach project focusing on the prediction of engine out NO_x by developing a semi-empirical 0D model which requires in-cylinder combustion parameters. This model is built basically to reduce both the cost and test cell timing, by requiring a smaller number of test data, while maintaining the predictability of the model at wider range of operating points, for the development and control purposes. In general, the NO_x emission model can be developed in different degrees of detail. The main approaches include 3D Computational Fluid Dynamics (CFD), 1D and 0D methods that can be classified by different degrees of detail and computational efforts. 3D CFD model [2]-[5] although predicts the NO_x emissions with high accuracy but requires a lot of computational time which is not suitable for developing models to focus on calibration and controls work. On the other hand, there are empirical models [6]-[9] which correlates NO_x emissions with the engine operating parameters, which are external to in-cylinder

Saurabh Sharma is with the Isuzu Technical Center of America, Plymouth, MI 48170 USA (corresponding author, e-mail: saurabh.sharma@isza.com).

Yong Sun and Bruce Vernham are with the Isuzu Technical Center of America, Plymouth, MI 48170 USA.

combustion, to generate a map-based model. These models are usually valid only for a narrow engine operating conditions at which they were fit with no predictive capability because they can interpolate but no extrapolate although these models take less computational time but require lot of test data points in order to calibrate the model. This provides a clear problem statement to answer how the model predictability can be increased while reducing the number of test points required to calibrate the model. The solution for this problem has been developed in this paper by considering the in-cylinder combustion physical parameter rather than looking at parameters which are outside combustion zone. By including these physical parameters, an effort has been made to capture the physics behind the NOx formation. Therefore, in this paper, an alternative solution has been used which accounts for the physics behind the NOx formation by choosing the in-cylinder combustion parameters and fitting them with the experimentally measured engine out NOx. The gist of this semi-empirical model is to estimate NOx emissions for a wide range of combustion and operating points and engine configuration with different hardware.

In order to choose the in-cylinder combustion parameters, it is necessary to understand the physics and chemistry involved in the NOx formation. NOx emissions are comprised of two chemical components: NO (70-95%) [10] and NO₂. Several mechanisms have been developed to explain the NO formation process by several ways: thermal path, NO-prompt, N₂O and NNH mechanisms. Among all the paths, thermal path is considered as main source of NO production by previous researchers. It is represented by Extended Zeldovich mechanism (EZM) reactions [11]:



The overall expression for the rate of NO formation results into the following equation [12]:

$$\frac{d[\text{NO}]}{dt} = \frac{6 \times 10^6}{T^{0.5}} \exp\left(-\frac{69,09}{T}\right) [\text{O}_2]_e^{0.5} [\text{N}_2]_e \quad (4)$$

where T is burn gas temperature (K), and [O₂]_e and [N₂]_e are the equilibrium concentration (mole/cm³) of oxygen and nitrogen respectively.

Equation (4) indicates that NOx formation is mainly dependent on the burn gas temperature and the oxygen concentration inside the combustion chamber, which means parameters related to equilibrium oxygen concentration and required temperature profile, should be important to build a model to predict engine-out NOx. Along with the high temperature, lean mixture region is also an important factor for the NOx formation [10]. Several semi-empirical models [13], [14] divided the combustion chamber into two zones which are burned and unburned zones and used the burned gas temperature for forming the NOx model, whereas Hegarty et

al. [15] focused on the temperature profile which is a function of mean in-cylinder combustion chamber temperature, adiabatic temperature and the heat release rate. Querel et al. [16], [17] estimated the temperature delta of burned and unburned regions and these models also examine the empirical sensitivity of NOx emissions to EGR and swirl in combustion chamber. The similar approach has been adopted by Savva et al. [18]. These models have shown a good correlation for the engine-out NOx but along with the high dependency on the input parameters.

There are several approaches which focus on developing correlations based on the measured NOx values on diesel engines. One of them is Wang et al. [19] where neural network models are developed by finding the empirical correlation between the parameters like engine speed, EGR rate, rail pressure, in-cylinder combustion temperature and air to fuel ratio. Saravanam et al. [20] studied the effect of fuel density, ignition delay and intake oxygen concentration. A polynomial model was developed between the parameters and the measured NOx emissions. Similar model structure was observed in Singh et al. [21] using a logarithmic correlation. They also studied the effects of fuel injection timing, quantity and pressure. Such kinds of models are used in control strategies and for OBD as virtual engine-out NOx sensor.

Based on this literature study, it is clear that the in-cylinder NOx formation is highly attached to the burned gas zone. Also, the EZM is a prominent model to measure physical NOx formation. But the non-linearity of equations and uncertainty in tabulated equilibrium concentrations complicate the construction of EZM model. Also, the Zeldovich mechanism only considers the thermal route and not the prompt NOx route. Therefore, a semi-empirical model is much easier to build, but that is only possible if right parameters are chosen. To fix these problems, the proposed model will replace the standard extended zeldovich model by a semi-empirical correlation between the in-cylinder combustion parameters and the measured NOx values. The proposed model highlights the necessary parameters which corresponds to the NOx formation and will also be attached to the key elements in the Zeldovich mechanism. The proposed model is the initial step of the development of the engine-out NOx model. The idea behind the building this model is to continuously develop the model as the engine development phase continues as shown in Fig. 1. Initially a small set of experimental data, traditionally from 3D CFD model, is used to build the cylinder level calibrated model. This cylinder level calibrated model is further developed to have a platform to perform component level validation and develop the base combustion and emission models. The developed combustion model is later converted to a multi-cylinder DI-pulse 1D-combustion model and at this point enough data points are collected to build and develop a semi-empirical model based on the physical in-cylinder combustion parameters. After validating the model at those available data sets, data from those operating points are then used to improve the model to predict the large set of DOE data. Therefore, it is a continuous development work with no termination point.

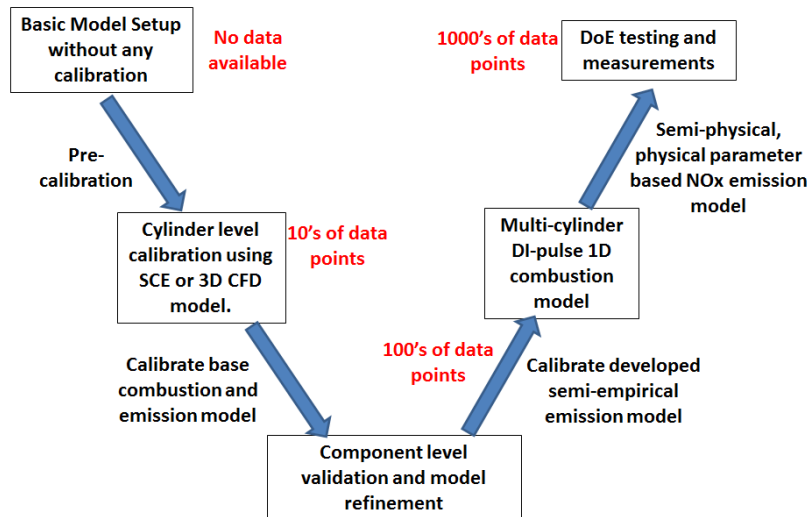


Fig. 1 V-cycle for the model development

II. ENGINE SETUP AND EXPERIMENTAL DATA

A medium heavy duty inline 4-cylinder diesel engine has been used to gather the engine-out NO_x data. It is equipped with single stage variable geometry turbocharger, charge air cooler, high pressure EGR, DOC, DPF, SCR and ASC systems. Data has been collected at various operating conditions as shown in Table I.

TABLE I
ENGINE DATA COLLECTED AT VARIOUS OPERATING CONDITIONS

Sno	Operation	Number of test points
1	Entire operating region data with EGR	138
2	Entire operating region data without EGR	123
3	EGR Sweep	39
4	Injection Sweep	77
5	VGT Sweep	48
6	VVT Sweep	21

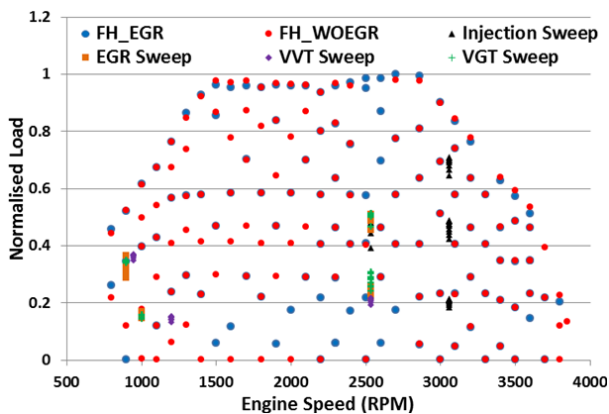


Fig. 2 Operating points at which data has been collected

Test points in Table I covered entire engine operating range and were represented regards to speed and fuel flow rate in Fig. 2. AVL CAMEO was used for test designs, automation

and data post-processing. To mimic the back pressure increase due to soot loading in DPF systems, all tests were performed with simulated back pressure in test cell using butterfly valve. Engine out emissions were measured using Horiba MEXA-7100 DEGR motor exhaust gas analyzer system; soot was measured by AVL MSS+. In-cylinder pressure trace, intake manifold pressure, exhaust manifold pressure and injection current signal were measured with respect to crank angle using AVL Indicom 621 system. EGR percentage was estimated with intake manifold CO₂ and O₂ measurement. AVL 300 kW AC dynamometer was used for all tests.

III. COMBUSTION MODEL

Before the emission model can be build, it is necessary to have a predictive cycle resolved combustion model which can simulate multiple combustion phases. This combustion model is required to provide all the relevant physical parameters that represent the physics behind the NO_x formation. It should be noted that the development of the combustion model was not the part of this work but a brief description and validation for the model will be provided in this work.

1D predictive engine models were developed using commercially available software GT-SUITE by Gamma Technologies Inc. The 1D detailed model development took 4 months to finish with time counting for data collection, components model development and validation. Faghani et al. [22] and Imran et al. [23] provided detailed explanation of model development and usage applications. Fig. 3 shows an overview of the detailed 1D engine model. Multi zone physical based combustion model, DI-Pulse, was used to accurately predict combustion physics [24], [25]. Multi-cylinder Three Pressure Analysis (TPA) approach was performed to calibrate and validate in-cylinder heat transfer, engine breathing and valve events [24], [26]. Woschni heat transfer model was setup in GT-Suite to capture in-cylinder heat transfer [10]. Map based friction model was implemented as function of engine speed and load. Detailed geometry-based

cylinder wall temperature solver was implemented to calculate heat losses to walls, liners, valves, cylinder block, oil and coolant. EGR valve position was controlled to target EGR percentage estimated from intake manifold CO₂ concentration measurement. Turbo vane position was controlled based on boost pressure target.

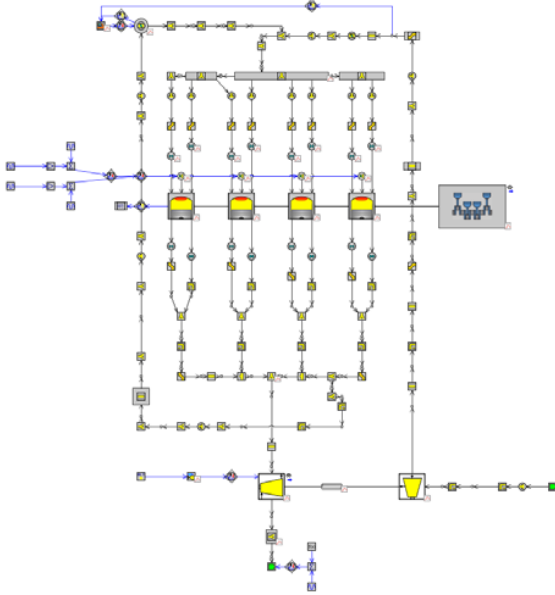


Fig. 3 Overview of detailed 1D engine model

TABLE II
ENGINE MODEL ACCURACY TARGETS

Sno	Parameter	Accuracy Targets
1	Brake Torque	± 5 %
2	EGR Percentage	± 1 % absolute difference
3	Brake Specific Fuel Consumption	± 5 g/kW-h
4	Air flow Rate	± 3 %
5	Peak Cylinder Pressure	± 5 Bar
6	Turbine Speed	± 5000 rpm
7	Exhaust side pressures	± 10 kPa
8	Exhaust side temperatures	± 20 °C
9	Intake side pressures	± 3 kPa
10	Intake side temperatures	± 5 °C
11	EGR valve position	± 5 % opening absolute difference
12	Turbo vane position	± 5 % opening absolute difference

For combustion modeling, 64 points from the operating region with EGR operation were picked to calibrate combustion rate and associated emissions. The predictive combustion calibration was carried out to minimize the RMS Error between simulated combustion burning rates and measured combustion burning rates. The burn rate RMS Error is defined as:

$$BR\ RMSE = \sqrt{\frac{(LHV_{sim} * BR_{sim} - BR_{exp})^2 dt}{t_{BRfinal} - t_{BRstart}}} \quad (5)$$

Table II illustrates other model accuracy targets. Turbocharger maps were implemented, and air path

predictions were validated using data of entire engine operation range without EGR. High pressure EGR path predictions were validated using EGR valve sweeps data.

Figs. 4-10 show detailed engine model validation plots for some important parameters. Accuracy bandwidth lines were shown correlating to those in Table II for better understanding of 1D detailed model accuracy validation plots.

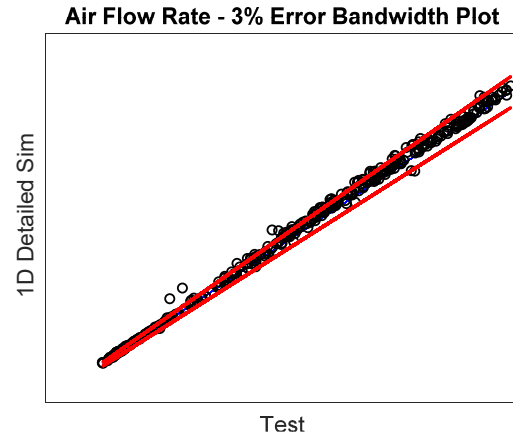


Fig. 4 Brake Torque prediction comparison

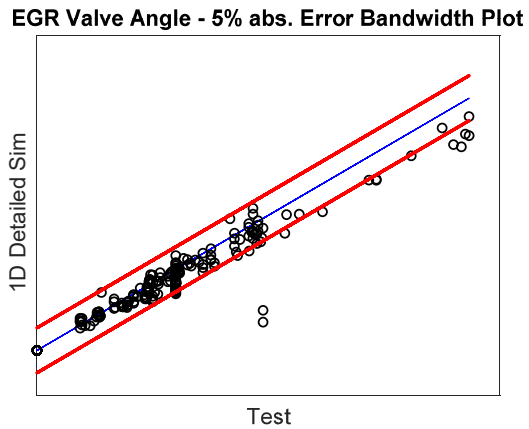


Fig. 5 EGR valve opening prediction comparison

In Fig. 4, the prediction trends were good for brake torque. Low brake torque was difficult to match due to solver instability and variation in EGR mixing between cylinders. Air mass flow rate in Fig. 6 was over-predicting because turbocharger efficiency maps were collected from gas benches and cannot fully replicate engine dyno operating heat transfer between turbine and compressor. Additionally, high speed and load intake charge air reheated the intake manifold and caused slight impact on volumetric efficiency and intake air charge temperature at low speed-low load conditions. Fig. 5 showed difference between intake throttle out temperature and intake manifold temperature measured on engine during low speed and load operating conditions for without EGR condition.

As observed in Fig. 8, for low load and speed points, intake manifold temperature was higher than intake throttle out

temperature, and the temperature difference between two locations became less for higher speed and load conditions. However, the prediction error of air mass flow rate remained within 5% error band.

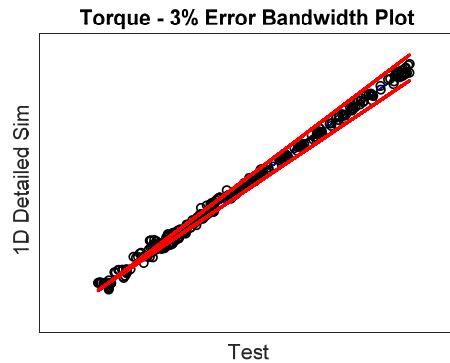


Fig. 6 Air mass flow rate prediction comparison

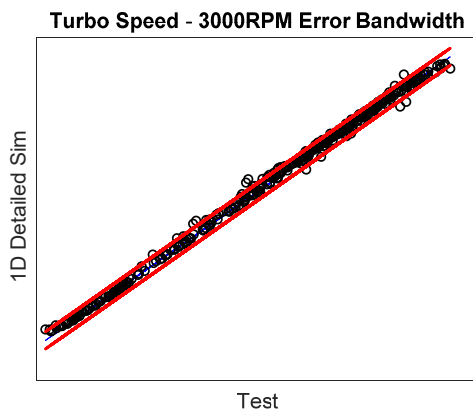


Fig. 7 Turbo speed prediction comparison

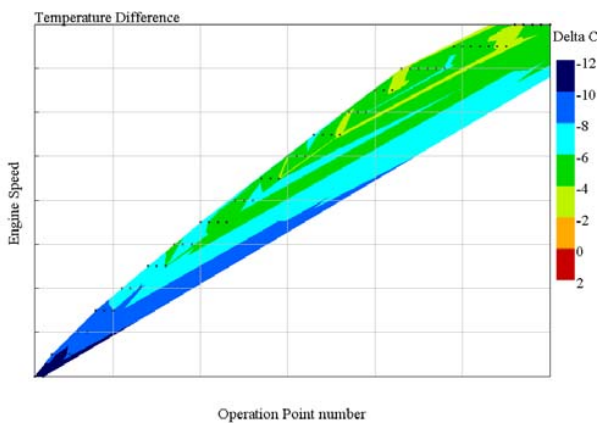


Fig. 8 Temperature difference Between Intake Throttle Out and Intake Manifold at low load low speed conditions

IV. MODEL DESCRIPTION

After going through the literatures, a brief discussion on the selection of parameters which have significantly high

influence on NO_x formation is hereby discussed. It is been observed from EZM reactions and the literature that the NO_x formation is highly dependent on the mixture temperature, fuel burn rate, production and consumption of O₂, N₂, O, N, H and OH species, charge air energy, fuel and air mixing frequency and the turbulence inside the combustion chamber. So, in order to study all these conditions, different in-cylinder combustion parameters are extracted from the detailed engine combustion model. In total, 260 parameters were selected such as maximum cylinder pressure rise rate, trapped fuel mass, combustion to motoring pressure ration, burnt oxygen concentration at different fuel burnt amount conditions to name a few.

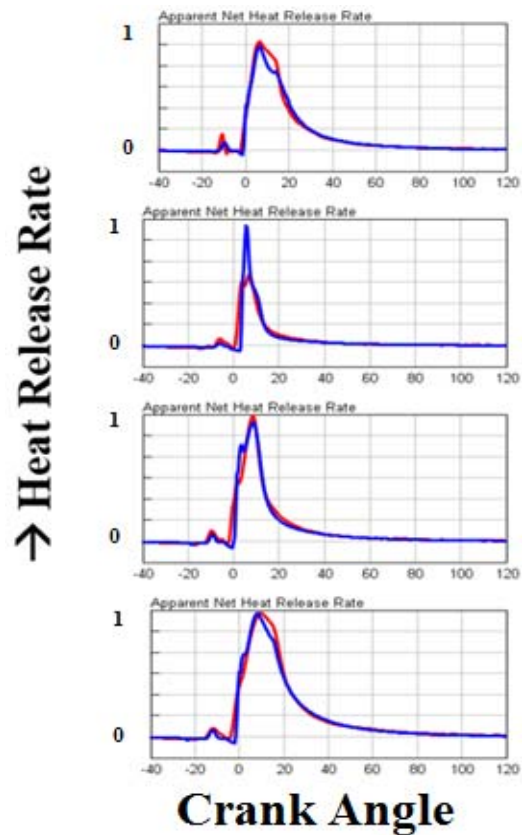


Fig. 9 Heat release rate prediction comparison

In Fig. 11, the correlation of all these parameters with respect to NO_x is shown, where x-axis is the spearman correlation number and on y-axis the parameters are listed in numeric number. Since the focus in this work is to have a predictive model with less number of calibration factors, the cutoff factor for the selection of the parameter was set to the spearman coefficient number of 0.7, as shown by dotted green line in Fig. 11. 28 parameters showed the correlation of higher than 0.7, which later being evaluated to check how high the inter-correlation between the parameter is there. Since the semi-empirical model is also a mathematical model, all the parameters should not be dependent on each other otherwise it will magnify the error in the model which is being brought by

individual physical parameter measured from the model. So, in order to keep the parameters independent to each other, a correlation number of 0.9 was set which should not be crossed during the inter-correlation analysis as reported in Fig. 12 for the finalized parameter. After the parameters are shortlisted from the inter-correlation analysis, based on the increment in the R^2 of model the parameters were added in the model and the selected parameters are listed in Table III, and a spearman correlation analysis of the selected parameters is shown in Fig. 13. All the parameters show correlation higher than 0.7. Also, the study for examining the co-products of the parameters is also conducted. In this study all the possible permutation and combination has been applied to study the improvement in the correlation with respect to measured NOx but at the same time correlation between the co-products is also kept below 0.9, as shown in Fig. 14.

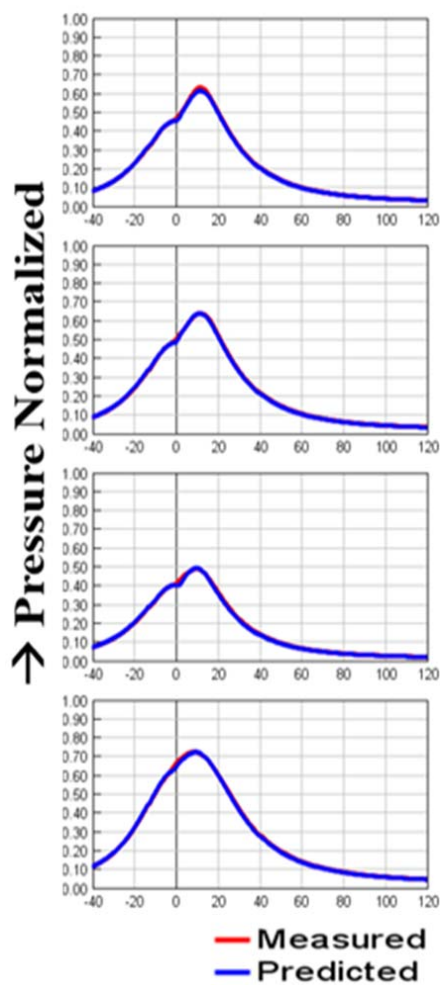


Fig. 10 Normalized pressure trace prediction comparison

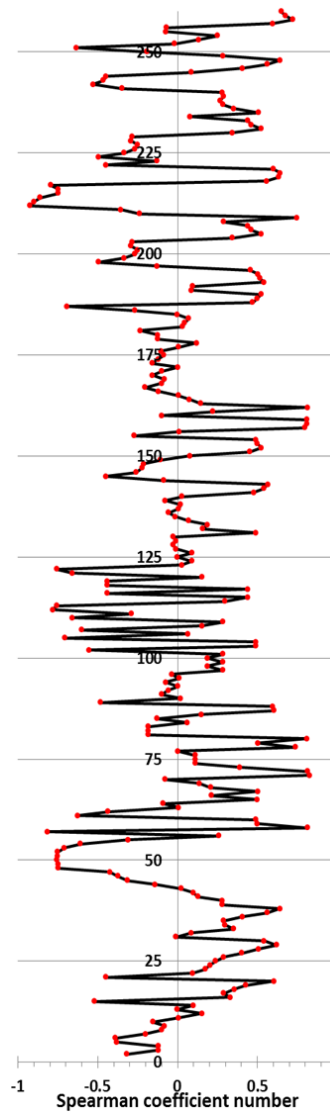


Fig. 11 Spearman correlation analysis of all the parameters

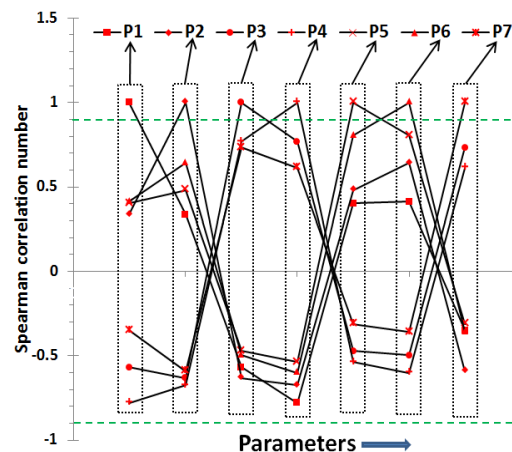


Fig. 12 Spearman correlation analysis of the inter-correlation of the selected parameters

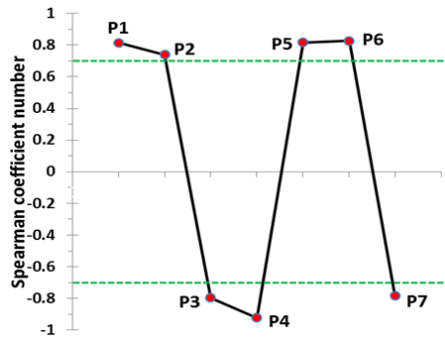


Fig. 13 Spearman analysis of the selected parameters with respect to NOx measurement

TABLE III
LIST OF SELECTED PARAMETERS

Sno	Parameter	Annotation
1	Peak burn gas temperature	P1
2	Peak average gas temperature	P2
3	O_2, p_1	P3
4	O_2, p_2	P4
5	Maximum pressure rise rate	P5
6	Combustion and motoring pressure ratio	P6
7	Trapped fuel mass	P7
8	$P5 \times P7$	P8
9	$P5 \times P4$	P9
10	$P6 \times P1$	P10
11	$P4 \times P2$	P11

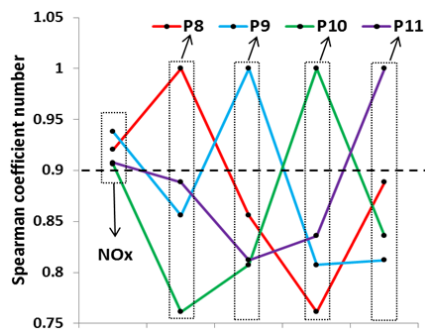


Fig. 14 Spearman analysis of the co-products of the parameters with respect to measured NOx

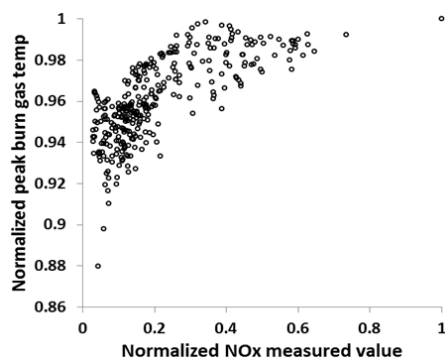


Fig. 15 Normalized peak burn gas temperature vs. normalized measured NOx value

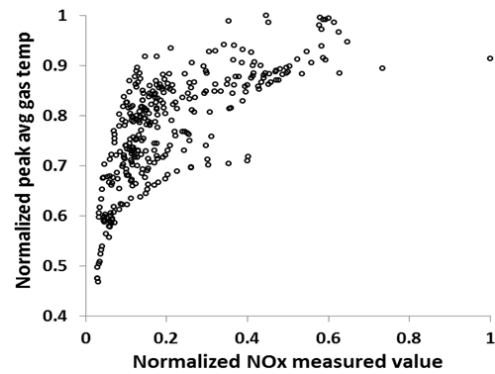


Fig. 16 Normalized peak average gas temperature vs. normalized measured NOx value

Hereafter the physical explanation of the selected parameters will be discussed. From (4), it is clearly observed that the burn gas temperature distribution plays an important role in the NOx calculation. Therefore, it should be included in the semi-empirical model. In the test also, it was observed that the peak burn gas temperature during the combustion has an exponential relationship with measured engine-out NOx as shown in Fig. 15. According to the Dec conceptual scheme [27], the NOx amount derived from thermal route is mostly formed in the stoichiometric diffusion flame. It can then proceed in the post-combustion region downstream from the diffusion flame. But the peak burn gas temperature represents only a very narrow region of high burn gas temperature. The rate of formation of NOx through thermal route is significant only at high temperatures (greater than 1800 K) because fixation of nitrogen requires the breaking of the strong nitrogen triple bond (dissociation energy of 941 kJ/gmol). So, in order to account for the overall air cylinder gas charge temperature, the peak of average gas temperature is also included in the model, and from Fig. 16 it can be observed that the measured NOx has a good exponential correlation with peak average gas temperature during the combustion.

Along with the gas temperature, oxygen concentration is also one of the important parameters which influence the NOx production, which was observed in (4). So, in order to account for the impact of oxygen on NOx formation, two parameters are included in this model. The first parameter (O_2, p_1) defines the total mass of oxygen burnt to achieve the peak burn gas temperature. The second parameter (O_2, p_2) is used to define how much oxygen mass has been burnt during the phase when the peak burn gas temperature drops from its peak value to 2000 K. These two parameters are also shown in Fig. 17 to give a clear pictorial view. O_2, p_1 captures the oxygen concentration being consumed in the NOx formation reactions during the first half of the combustion, i.e. before the adiabatic flame temperature is achieved. When the temperature starts to drop down, the NOx formation phenomenon at high temperature is captured by O_2, p_2 . Figs. 18 and 19 also show that the two parameters defining impact of O_2 has good correlation which measured NOx.

The mass of N_2 and O_2 which are available inside the

combustion chamber in diffusive burned gas region is proportional to the fuel mass burn rate. With the high fuel burn rate, high combustion pressure rise rate is observed, so pressure rise rate can be used as the rate of fuel burnt. Also, the Fig. 20 shows good correlations between the maximum pressure rise rate and the measured NOx, therefore this term should be included in the model. Along with the fuel burn rate, the rise in the air charge energy inside the combustion chamber also plays an equal important role for generating NOx. This change in the air charge energy can be indicated by looking at the ratio between the max pressure obtained during combustion and motoring period. Fig. 21 confirms this hypothesis by showing the expectable trend line between the measured NOx and the combustion and motoring pressure ratios.

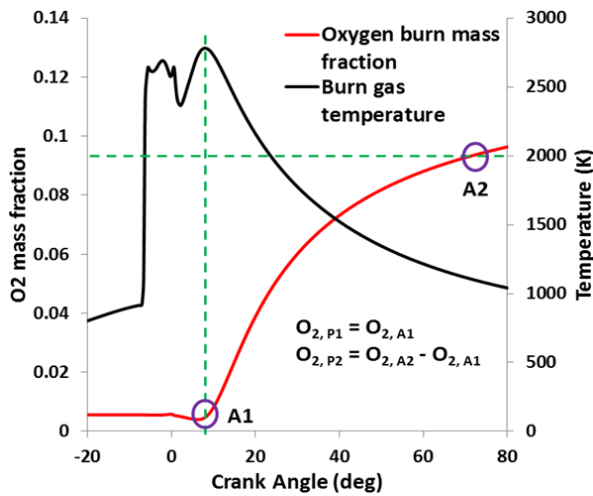


Fig. 17 Definition of $O_{2,P1}$ and $O_{2,P2}$

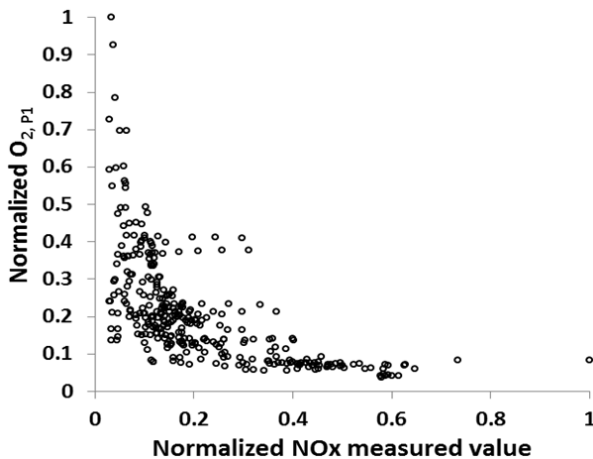


Fig. 18 Normalized $O_{2,P1}$ vs normalized measured NOx value

With the given parameters such as pressure ratio and pressure rise rate, the fuel burn rate has been taken care of but the fuel which is being trapped inside the cylinder has also to be considered. This is due to the fact that the NOx is majorly formed in diffusion flame region, and the trapped fuel mass

can lead to a small premixed combustion region which results in the lower NOx generation. Fig. 22 also supports this hypothesis and shows a clear correlation between trapped fuel mass and the measured NOx.

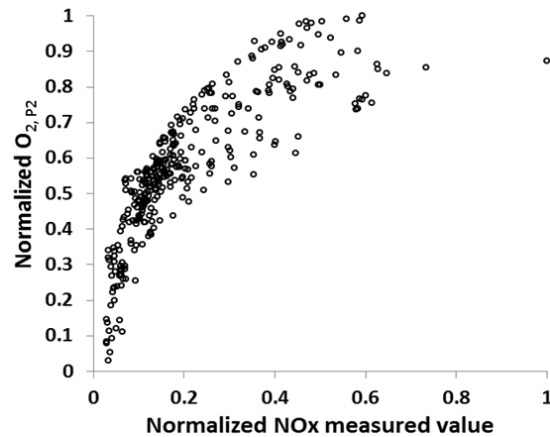


Fig. 19 Normalized $O_{2,P2}$ Vs normalized measured NOx value

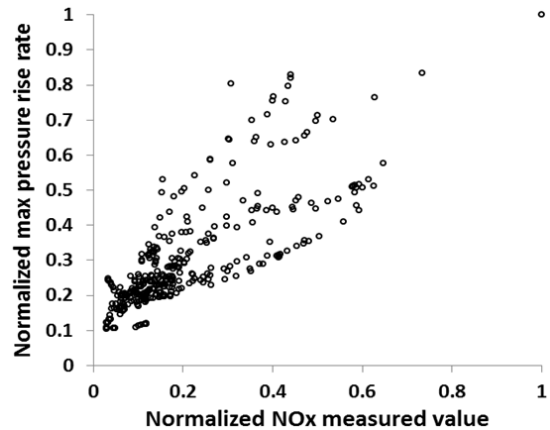


Fig. 20 Normalized max pressure rise rate Vs normalized measured NOx value

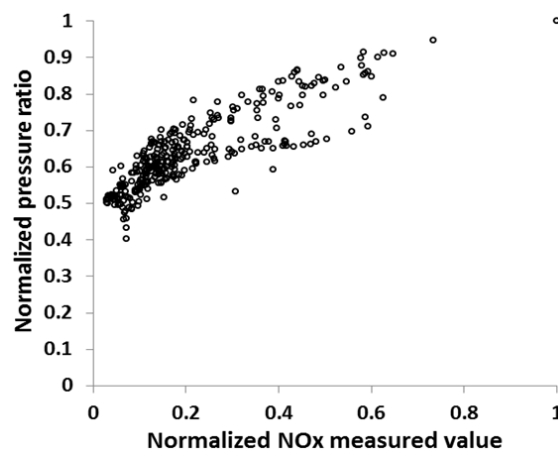


Fig. 21 Normalized max combustion and motoring pressure ratio Vs normalized measured NOx value

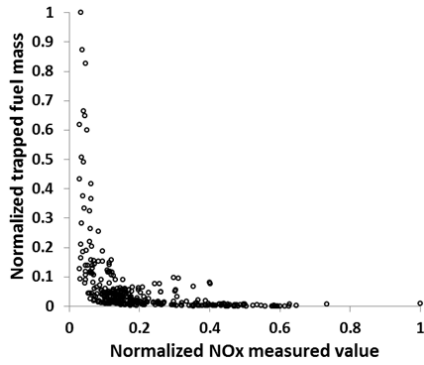


Fig. 22 Normalized trapped fuel mass Vs normalized measured NOx value

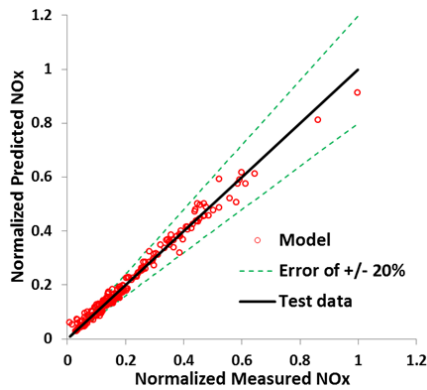


Fig. 23 Predicted Vs measured NOx emissions comparison for the calibration data set

V. RESULTS AND DISCUSSION

On the basis of the discussion in above section, the engine-out NOx concentration should be function of the parameters given in Table III, and the following function form has been proposed:

$$NOx (PPM) = A_1 + A_2 X(e^{B_1 X P_1}) + A_3 X(e^{B_2 X P_2}) + A_4 X P_3^{B_3} + A_5 X(e^{B_4 X P_4}) + A_6 X P_5 + A_7 X P_6 + A_8 X P_7^{B_5} + A_9 X P_8 + A_{10} X P_9 + A_{11} X P_{10} + A_{12} X P_{11} \quad (6)$$

where A_1 - A_{12} and B_1 - B_5 are the calibration factors and the exponential powers are determined by the mathematical relationship which was observed between the parameters and the measured NOx. The proposed equation has been calibrated by means of the least square method, on the basis of the steady state data mentioned in Table I. This has allowed the calibration factors to be successfully calibrated. It should be noted that only half of the data was used to calibrate the model the rest of the half was purely used to validate the model. Also, the data selection was randomly to avoid any human biasness. The calibrated model shows a good fit as shown in Fig. 23. The error line of +/- 20% is also plotted to give any idea of the range in which the prediction is matching with experimental data. From the plot it is clear that almost all of the data lies within the region with a RMSE of 74 PPM, nRMSE of 2.26% and the coefficient of determination R^2 of

0.985.

Now the rest of the half of data was used to predict the NOx concentration and as shown in Fig. 24, almost all the predicted points are within the error limits with a RMSE of 78 PPM, nRMSE of 2.25% and the R^2 of 0.9814. It can be observed that the correlation and the RMSE of the calibrated and validated data are very close which signifies that model is well calibrated and have good predictability.

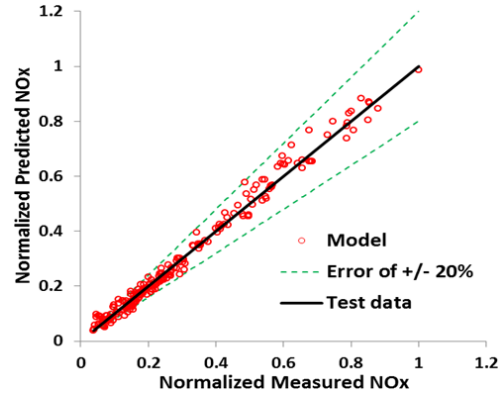


Fig. 24 Predicted Vs measured NOx emissions comparison for the validation data set

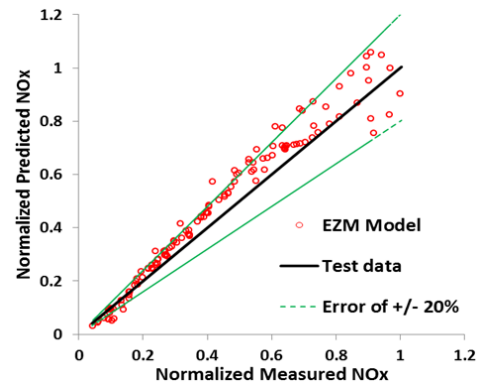


Fig. 25 Predicted Vs measured NOx emissions comparison for the EZM model for with EGR operating region data

The developed semi-empirical model is then compared with the EZM model and as it is shown in Fig. 25 that in the entire operating region with EGR, the model is able to predict the NOx concentration with a RMSE of 168 PPM, nRMSE of 7.34% and the R^2 of 0.96. The high RMSE is due to the larger percentage of error in high NOx region, which has been improved significantly in the proposed semi-empirical model. Similar observation is captured when the NOx concentration was calculated in no EGR cases, where RMSE, nRMSE and R^2 are 111 PPM, 4.88% and 0.9753 respectively, as shown in Fig. 26.

Further model prediction capability was tested by using the model to predict NOx for the different sweep cases such as EGR, VGT and injection sweep. As shown in Fig. 27, in the injection sweep data set, the model was able to predict the NOx with nRMSE of 2.05% and the R^2 of 0.99. Similarly, for

EGR and VGT sweep test, the model was predicting well with the 20% error limit with the nRMSE of 4.16% and 4.71% respectively as shown in Figs. 28 and 29. Although the semi-empirical model (UDF) shows lower predictability in the case of EGR and VGT sweep but when compared with the results got from the EZM model, the UDF model shows much better prediction at higher NO_x region. Since there is issue with the prediction in EZM model also, the combustion model must be checked at the given sweeps.

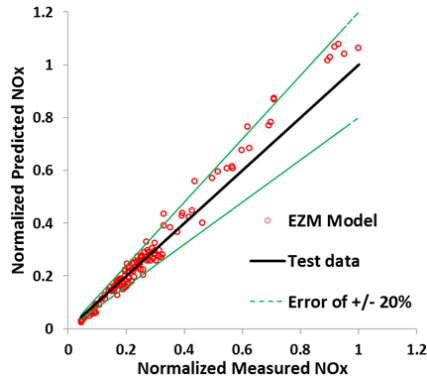


Fig. 26 Predicted Vs measured NO_x emissions comparison for the EZM model for without EGR operating region data

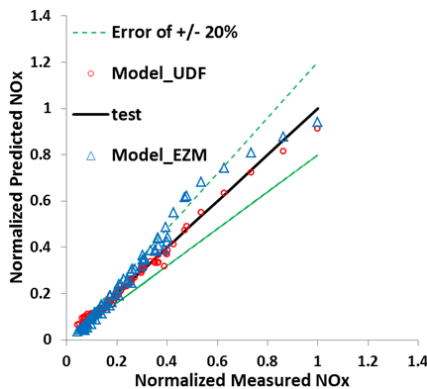


Fig. 27 Predicted Vs measured NO_x emissions comparison for the injection sweep data set

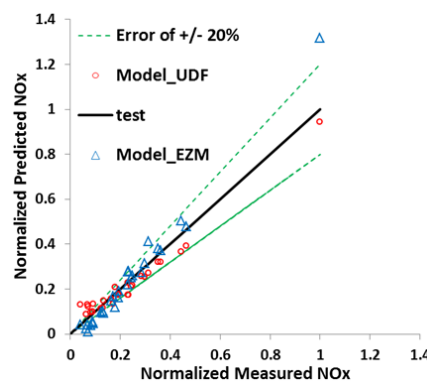


Fig. 28 Predicted vs. measured NO_x emissions comparison for the EGR sweep data set

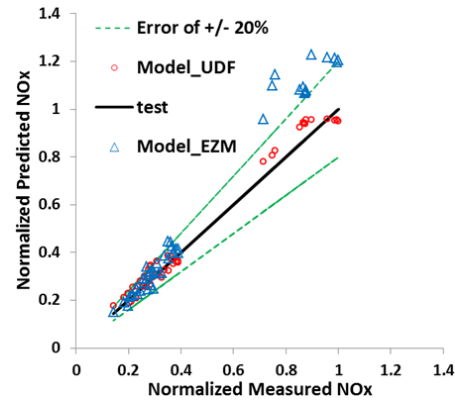


Fig. 29 Predicted Vs measured NO_x emissions comparison for the VGT sweep data set

To further validate the developed model, data was collected at completely different engine and that data was used to predict the NO_x concentration. As shown in Fig. 30, the NO_x concentration is predicted with a RMSE of 91 PPM, nRMSE of 6.32% and R^2 of 0.865. The model has a linearly over prediction trend, but it should be noted that the NO_x has been calculated with the same model and without recalibrating the factors for this engine. Most of the data was within 20% error bandwidth but few of the data was also distributed between 20 to 35% error zone and couple of points with error higher than 35%. Model is able to predict significantly better at lower NO_x region compared to the higher NO_x concentration region. After recalibrating the model with 50% of the data available for this engine, the model accuracy drastically improved and the NO_x concentration is now well predicted with the RMSE of 50 PPM, nRMSE of 3.5% and R^2 of 0.92, as shown in Fig. 31.

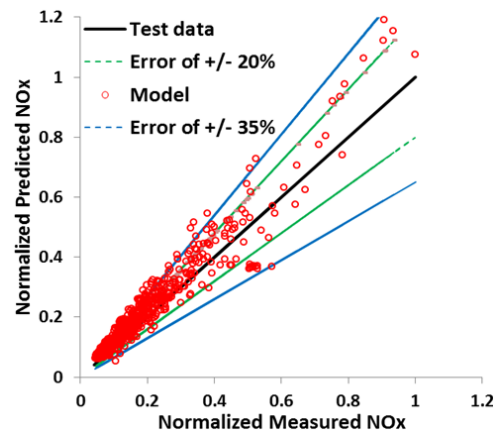


Fig. 30 Predicted vs. measured NO_x emissions comparison for the completely different engine data set without recalibrating the model

In the literature review, it was observed that the machine learning approach for making the model is only another model calibrating method, therefore it will require the same amount of data to calibrate the model based on the physical parameters. So, in this work, an effort was also made to check

how the neural network model behaves with the smaller number of data points but with the physical parameters which represents the physics behind NO_x formation. Several algorithms were tested and the RMSE results show that with the availability of 75% data set for calibration, model was able to predict the NO_x with the RMSE of as low as 58.6 PPM as shown in Table IV. It was observed that SVM model provides good correlation compared to the other methods especially super learner. In the super learner approach the percentage of contribution of gbm, random forest, polymars and svm is 5.5%, 28.3%, 40.6% and 25.6% respectively. It should be also noted that the super learner result reported in this work is obtained after n-fold cross validation, example is shown in Fig. 32, whereas there is no cross validation for SVM approach. This shows that the different results can be obtained by choosing different regression model, but the important part in building a semi-empirical model is the selection of the parameters which have physical or chemical relationship with the NO_x formation. It is also important to focus on the complexity of the model. Since it is difficult to integrate a machine learning model or neural network model with the combustion model of GT-Power, a simple mathematical function is chosen to represent the NO_x formation which can be easily integrated as a mathematical function and will not impact the run time of the current combustion model.

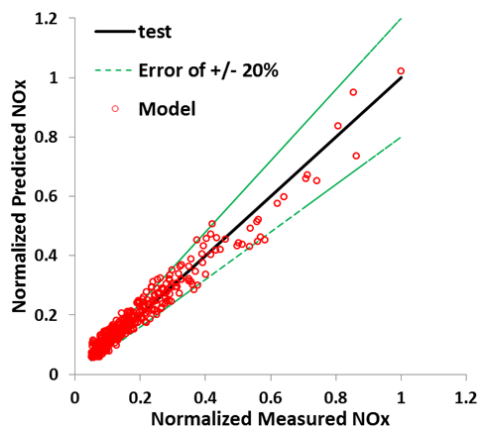


Fig. 31 Predicted Vs measured NO_x emissions comparison for the completely different engine data set after recalibrating the model

TABLE IV
RMSE RESULTS FROM DIFFERENT ALGORITHMS

Sno	Algorithm	RMSE for 25% data set validation
1	Support Vector Machine (SVM)	58.6
2	Random Forest	85.245
3	Super Learner	85.342
4	Polymars	170.8114
5	gbm	87.5706

VI. CONCLUSION

This work presented the development and validation framework of a semi-empirical zero-dimensional NO_x model for the medium heavy duty diesel engine. The model is based

on the physical in-cylinder combustion parameters which defines the physics and chemistry behind the NO_x formation. The selection of these parameters is then combined with empirical model with the available data points. To achieve the target, three major objectives have been achieved:

- 1) A predictive combustion model should be developed, so that the in-cylinder parameters can be extracted.
- 2) Second step is to ensure the selected parameters have physical relationship with NO_x test data and does not have high inter-correlation. The high inter-correlation will lead to the higher chance of error increment in the model which is being brought by the parameters taken from the combustion model.
- 3) With the availability of advanced regression tool, a final linear NO_x model was built as a function of physical parameters. The summary of the results of the accuracy of the model for different test conditions is presented in Table V.



Example: 5-fold cross validation

Fig. 32 Example of n-fold cross validation approach

TABLE V
RMSE RESULTS FROM DIFFERENT ALGORITHMS

Sno	Test condition	RMSE (PPM)	nRMSE (%)	R ²
1	Calibration at operating condition	74	2.26	0.985
2	Validation at operating condition	78	2.25	0.9814
3	EZM prediction operating condition with EGR	168	7.34	0.96
4	EZM prediction operating condition without EGR	111	4.88	0.9753
5	Model prediction at injection sweep	72	2.05	0.99
7	Model prediction at EGR sweep	70	4.16	0.9687
8	Model prediction at VGT sweep	75	4.71	0.9837
9	Engine 2 validation without re-calibration	91	6.32	0.865
10	Engine 2 validation with re-calibration	50	3.5	0.92

Validation results show that the developed model is able to predict the NO_x concentration with high accuracy especially for the lower and middle range of NO_x values. The accuracy was slightly off at higher NO_x values when the model was test on different engine data set. Overall the results were within the

tolerance limit and with the advantage of lower computational time and cost; it can have a meaningful contribution in achieving a virtual engine platform which can be used for multiple applications such as control strategies development, engine pre calibration and HIL testing.

It should be noted that this is not the end of the proposed semi-empirical model. The model has been developed based on the initial small amount of data set. It has to be tested and then calibrated for the wide range of design of experiments (DOE) data sets to make it more robustness and predictable. This model will be used to form another level of model which will be used in future development work. This continuous improvement and development will be done by using the data from other set of NTE (not to exceed) and altitude testing where the model has already been used for predicting the engine-out NO_x emission. Based on the discussion in this paper, the following future work has been planned:

- 1) Similar approach will be used to model other emission models such as soot, CO and HC but most of the efforts should be spent on selecting the physical parameters which can have huge impact on the model's predictability. This requires the automation of the parameter selection based on domain expert knowledge instead of purely data driven.
- 2) Machine learning aided formula can be constructed which will require fewer manual efforts and can find more representative formula for the mathematical function to integrate in the combustion model.
- 3) Sensitivity analysis will be performed to determine the impact of error percentage inside the parameter on the overall model prediction error. A systematic approach has to be determined to reduce the impact of the parameter uncertainty.
- 4) Finally, a deterministic deep learning and machine learning approach has to be developed to improve model predictability and robustness.

REFERENCES

- [1] Finesso, R., Marelli, O., Misul, D., Spessa, E. et al., "Development and Assessment of Pressure-Based and Model-Based Techniques for the MFB50 Control of a Euro VI 3.0L Diesel Engine," SAE Int. J. Engines 10(4):2017, doi:10.4271/2017-01-0794.
- [2] Pariotis, E. and Hountalas, D., "A New Quasi-Three Dimensional Combustion Model for Prediction of DI Diesel Engines' Performance and Pollutant Emissions," SAE Technical Paper 2003-01-1060, 2003, <https://doi-org.proxy.lib.umich.edu/10.4271/2003-01-1060>.
- [3] Mobasher, R., Peng, Z., Mirsalim, S.M., "Analysis the effect of advanced injection strategies on engine performance and pollutant emissions in a heavy duty DI-diesel engine by CFD modeling", International Journal of Heat and Fluid Flow 33:59-69, 2012, doi: 10.1016/j.ijheatfluidflow.2011.10.004.
- [4] O'Connor, J., White, C., and Charnley, M., "Optimising CFD Predictions of Diesel Engine Combustion and Emissions Using Design of Experiments: Comparison with Engine Measurements," SAE Technical Paper 982458, 1998.
- [5] Verma, I., Meeks, E., Bish, E., Kuntz, M. et al., "CFD Modelling of the Effects of Exhaust Gas Recirculation (EGR) and Injection Timing on Diesel Combustion and Emissions," SAE Technical Paper 2017-01-0574, 2017, <https://doi-org.proxy.lib.umich.edu/10.4271/2017-01-0574>.
- [6] Ericson, C., Westerberg, B., and Egnell, R., "Transient Emission Predictions With Quasi Stationary Models," SAE Technical Paper 2005-01-3852, 2005, doi:10.4271/2005-01-3852.
- [7] Subramaniam, M., Tomazic, D., Tatur, M., and Laermann, M., "An Artificial Neural Network-based Approach for Virtual NO_x Sensing," SAE Technical Paper 2008-01-0753, 2008, doi:10.4271/2008-01-0753.
- [8] Sequenz, H., Isermann, R., "Emission Model Structures for an Implementation on Engine Control Units", In Proc. Of the 18th IFAC World Congress, Milano, Italy, Aug. 28 - Sept. 2, 2011, doi:10.3182/20110828-6-IT-1002.03131.
- [9] Hashemi, N., Clark, N.N., "Artificial neural network as a predictive tool for emissions from heavy-duty Diesel vehicles in Southern California", International Journal of Engine. Research. 8(4):321-336, 2007, doi: 10.1243/14680874JER00807.
- [10] Heywood, J. B., "Internal Combustion Engine Fundamentals," McGraw-Hill Book Company, 1988.
- [11] Lavoie, G. A., Heywood, J. B., and Keck, J. C., "Experimental and Theoretical Study of Nitric Oxide Formation in Internal Combustion Engines," Combustion Science and Technology, vol. 1, pp. 313-326, 1970.
- [12] Lee, J., Lee, S., Park, W., Min, K. et al., "The Development of Real-time NO_x Estimation Model and its Application," SAE Technical Paper 2013-01-0243, 2013, doi:10.4271/2013-01-0243.
- [13] Lebas, R., Fremovici, M., Font, G., and Le Berr, F., "A Phenomenological Combustion Model Including In-Cylinder Pollutants To Support Engine Control Optimisation Under Transient Conditions," SAE Technical Paper 2011-01-1837, 2011, doi:10.4271/2011-01-1837.
- [14] Walke, N., Marathe, N., and Nandgaonkar, M., "Simplified Combustion Pressure and NO_x Prediction Model for DI Diesel Engine," SAE Technical Paper 2013-26-0131, 2013, doi:10.4271/2013-26-0131.
- [15] Hegarty, K., Favrot, R., Rollett, D., and Rindone, G., "Semi-Empiric Model Based Approach for Dynamic Prediction of NO_x Engine Out Emissions on Diesel Engines," SAE Technical Paper 2010-01-0155, 2010, doi:10.4271/2010-01-0155.
- [16] Querel, C., "Modélisation des émissions de NO_x pour le contrôle des moteurs diesel," Rouen: Université de Rouen, 2013.
- [17] Quérel, C., Grondin, O., and Letellier, C., "A Semi-Physical NO_x Model for Diesel Engine Control," SAE Technical Paper 2013-01-0356, 2013, doi:10.4271/2013-01-0356.
- [18] Savva, N. and Hountalas, D., "Detailed Evaluation of a New Semi-Empirical Multi-Zone NO_x Model by Application on Various Diesel Engine Configurations," SAE Technical Paper 2012-01-1156, 2012, doi:10.4271/2012-01-1156.
- [19] Wang, Y., He, Y., and Rajagopalan, S., "Design of Engine- Out Virtual NO_x Sensor Using Neural Networks and Dynamic System Identification," SAE Int. J. Engines 4(1):837-849, 2011, doi:10.4271/2011-01-0694.
- [20] Saravanan, S., Nagarajan, G., Anand, S., and Sampath, S., "Correlation for thermal NO_x formation in compression ignition (CI) engine fuelled with diesel and biodiesel," Energy, vol. 42, pp. 401-410, 2012.
- [21] Singh, N., Nagabushan-Venkatesh, P., Nigro, E., and Lack, A., "Development of the NO_x Emission Model for the Heavy Duty Diesel Engine Application Using Combustion Characteristic Parameters," SAE Technical Paper 2013-01-0532, 2013, doi:10.4271/2013-01-0532.
- [22] Faghani, E., Andric, J., and Sjoblom, J., "Toward an Effective Virtual Powertrain Calibration System," SAE Technical Paper 2018-01-0007, 2018, doi:10.4271/2018-01-0007.
- [23] Cosadia, I., Silvestri, J., Papadimitriou, I., Maroteaux, D. et al., "Traversing the V-Cycle with a Single Simulation - Application to the Renault 1.5 dCi Passenger Car Diesel Engine," SAE Technical Paper 2013-01-1120, 2013.
- [24] Engine performance application manual, GT SUITE, Gamma Technologies.
- [25] Piano, A., Mollo, F., Boccardo, G., Rafigh, M. et al., "Assessment of the Predictive Capabilities of a Combustion Model for a Modern Common Rail Automotive Diesel Engine," SAE Technical Paper 2016-01-0547, 2016.
- [26] Lakshmidhar, U., "Multi-Cylinder TPA and DI-Pulse Model development using GT-SUITE" GT Conference NA 2017.
- [27] Dec, J., "A Conceptual Model of DI Diesel Combustion Based on Laser-Sheet Imaging*," SAE Technical Paper 970873, 1997, <https://doi-org.proxy.lib.umich.edu/10.4271/970873>.